Cancer Cell
Article

A Functional Role for Tumor Cell Heterogeneity in a Mouse Model of Small Cell Lung Cancer

Joaquim Calbo,[1,3,4] Erwin van Montfort,[1,3] Natalie Proost,[1] Ellen van Drunen,[2] H. Berna Beverloo,[2] Ralph Meuwissen,[1,5] and Anton Berns[1,*]
[1]Division of Molecular Genetics and Center of Biomedical Genetics, Netherlands Cancer Institute, 1066 CX Amsterdam, The Netherlands
[2]Department of Clinical Genetics, Erasmus University Medical Center, 3000 CA Rotterdam, The Netherlands
[3]These authors contributed equally to this work
[4]Present address: Metabolic Engineering and Diabetes Therapy Lab., Institute for Research in Biomedicine (IRB Barcelona), 08028 Barcelona, Spain
[5]Present address: Centre Recherche INSERM U823 Equipe 2, Institut Albert Bonniot 38706 La Tronche Cedex, Grenoble, France
*Correspondence: a.berns@nki.nl
DOI 10.1016/j.ccr.2010.12.021

SUMMARY

Small cell lung cancer (SCLC) is the lung neoplasia with the poorest prognosis, due to its high metastatic potential and chemoresistance upon relapse. Using the previously described mouse model for SCLC, we found that the tumors are often composed of phenotypically different cells with either a neuroendocrine or a mesenchymal marker profile. These cells had a common origin because they shared specific genomic aberrations. The transition from neuroendocrine to mesenchymal phenotype could be achieved by the ectopic expression of oncogenic Ras^{V12}. Crosstalk between mesenchymal and neuroendocrine cells strongly influenced their behavior. When engrafted as a mixed population, the mesenchymal cells endowed the neuroendocrine cells with metastatic capacity, illustrating the potential relevance of tumor cell heterogeneity in dictating tumor properties.

INTRODUCTION

Small cell lung cancer (SCLC) accounts for 15%–20% of newly diagnosed lung malignancies, and is defined by neuroendocrine differentiation and small cell morphology of the tumor cells. SCLC is the deadliest and most aggressive type of lung cancer, mainly due to the early tumor cell dissemination and the almost invariable recurrence of chemoresistant lesions after chemotherapy (Jackman and Johnson, 2005). Tumors initially treated successfully by chemotherapy recur as chemoresistant variants and occasionally show progression to a non-SCLC (NSCLC) phenotype (Abeloff et al., 1979), suggesting the rapid selection of preexisting chemoresistant cell clones. Tumor cell dissemination and metastasis appear to be common, relatively early events in SCLC. The metastatic capacity could be an intrinsic feature of neuroendocrine SCLC cells or reflect the specific characteristic of a rare cell population present in tumors. Unfortunately, studies with archival patient material have not resolved this, and the factors critical for metastatic spread during SCLC progression remain elusive. Research on SCLC has been hampered by poor access to primary tumor material due to late detection of tumors, making this tumor inoperable in the vast majority of cases. In this situation, cell lines are the primary research tool, although their utility is limited by genetic drift and selection as a result of serial passaging in vitro with the concomitant loss of intra-tumor heterogeneity. Furthermore, most human SCLC cell lines were obtained from metastatic sites or from pleural effusions (Carney et al., 1985a) and will unlikely retain the cellular composition of the primary tumor mass.

Intra-tumor heterogeneity with respect to cell morphology but also proliferation rate, ability to metastasize, sensitivity to drugs, dependence on growth signals, and tumor initiation/repopulation capacity have since long been recognized as a salient feature of most malignancies. Tumor masses also harbor a range

Significance

It is increasingly realized that during tumorigenesis a variety of cells are recruited into the tumor to provide a range of functions that are associated with tumor progression. Weinberg and colleagues showed that mesenchymal stem cells recruited into the stroma of breast tumors promote metastasis through CCL5-mediated paracrine signaling, thereby emphasizing the relevance of the interactions between tumor cells and the surrounding microenvironment. The work presented here is in full agreement with this concept but adds an important component: the mesenchymal compartment of the tumor in our system is generated from a separate subclone during the tumorigenic process, providing the tumor cell population as a whole with new capabilities such as metastatic potential.

of normal cell types (stromal and infiltrating cells). The interactions between these different cell types can be critical for tumor development (Condeelis and Pollard, 2006; de Visser et al., 2006; Kalluri and Zeisberg, 2006). One particular example of such interactions was recently reported by Karnoub and collaborators (Karnoub et al., 2007): mesenchymal stem cells recruited into the stroma of breast tumors promote metastasis through CCL5-mediated paracrine signaling. However, the term "tumor heterogeneity" is primarily used to denote the diversity observed in tumor cells themselves, often marked by distinct genetic and epigenetic alterations (Heppner, 1984). Two current concepts attempt to explain the variations in cell morphology and behavior observed in tumors: the cancer stem cell hypothesis, and the clonal evolution model (Campbell and Polyak, 2007). Although these two concepts are mutually exclusive when strictly interpreted, an intermediate model including features of each hypothesis might fit best the actual observations. Mutation and clonal expansion may generate cells with stem cell properties, being able to self-renew and differentiate while also accumulating new mutations that give rise to diverse cell lineages in a tumor. Although tumor heterogeneity is a recurrent feature of most tumors, and its origins are now becoming understood, one important question has remained unanswered: does tumor cell heterogeneity fulfill a direct functional role, or has it little effect on tumor properties except for providing a reservoir of variant cells that permit swift adaptation to altered conditions, such as exposure to cytotoxic drugs. Work from Heppner's laboratory (Heppner, 1993) in the 1970s and 1980s pointed to a very interesting possibility: cell variants in a tumor interact with each other, resulting in societal behaviors that cannot be predicted by studying the properties of pure cell populations. However, the research focus has shifted more toward the identification of those tumor cells that have the capacity to reconstitute a tumor (Gangemi et al., 2009; Rosen and Jordan, 2009; Visvader and Lindeman, 2008). We decided to study to what extent tumor heterogeneity in SCLCs affects the properties of the tumor cell population as a whole.

Previously, we have described a mouse model for SCLC (Meuwissen et al., 2003) that shows many of the salient features of human SCLC (Minna et al., 2003). Keeping in mind that "tumor heterogeneity is a sort of written history of a particular cancer from which we can learn" (Campbell and Polyak, 2007), we focused on the identification of cell variants, with the objective of establishing genotype-phenotype correlations (Calbo et al., 2005). We now describe their clonal relationship and propose a model for their generation. Moreover, by conducting in vitro and in vivo mixing experiments, we address whether the cross-talk between these variants can alter their properties.

RESULTS

Mouse SCLC Tumors Contain Different Tumor Cell Populations

To extend the characterization of murine SCLC (Meuwissen et al., 2003), tumors obtained from 21 mice were dissected, disaggregated, and cultured in modified HITES medium (Linnoila et al., 1993). In all cases, tumor cells expanded rapidly and could be cultured for extended periods of time. Primary cultures derived from histology-confirmed SCLC tumors grew as suspensions of small aggregated cells. However, nine of the 21 cultured tumors also showed cells that attached to the dish. This is consistent with cell cultures derived from human SCLC tumors (Carney et al., 1985a).

Given the morphological heterogeneity in the cultured cells, single-cell suspensions from 15 of the above mentioned cultures were seeded in soft agar-containing medium, and individual colonies were isolated and expanded separately. Most of the obtained clones grew as suspending aggregates of very small cells. A similar cellular size and morphology were observed in a small proportion of adherent cell clones, with cells growing in clusters or very dense colonies and showing no spreading. However, other clones grew as a cellular monolayer composed of larger cells with visible cytoplasm and spindle-like membrane extensions, spreading on the substrate. Clones growing as suspending aggregates were found in all the tumors assayed, whereas 40% of the same tumors (six out of 15) also gave rise to clones with adherent, large cell phenotype (Figure 1A; see Tables S1 and S2 available online). Next, we asked whether SCLC-derived clones expressed markers of neuroendocrine differentiation. Cells growing as suspending aggregates did express variable amounts of neuroendocrine protein markers, as shown in Figure 1B for synaptophysin (Syp), achaete-scute complex homolog 1 (Ash1), and neural cell adhesion molecule (NCAM). By contrast, cells with the large cell phenotype did not show expression of Syp and Ash1, while expressing relatively low levels of NCAM. Of note, these cells showed two discrete forms (120 and 180 kDa) of NCAM in western blot, whereas the small cells growing in suspension showed smeared bands likely related to the characteristic polysialylation of NCAM protein (Hildebrandt et al., 2008; Lantuejoul et al., 1998). Six paired cell lines (small cell phenotype/large cell phenotype) derived from six independent tumors and three additional small cell clones were subjected to expression profiling using oligonucleotide-based microarrays. As controls, one cell line obtained from a histology-confirmed NSCLC and normal lung were included in the analysis. Principal component analysis (PCA) showed the clustering of samples into two groups: one containing small cell clones from independent SCLC tumors, and another containing large cell clones from different SCLC tumors. Interestingly, when the three principal components were shown in a 3D representation (Figure 1C), the large cell cluster was relatively close to the NSCLC sample, whereas the small cell cluster was far away, indicating a larger difference in overall expression profile. A total of 4239 genes were differentially expressed between small cell and large cell clones. From those the 20 most upregulated and the 20 most downregulated genes were selected to generate a small cell versus large cell signature (Figure S1A). The most significant biological functions associated with the small cell versus large cell upregulated genes, as identified by Ingenuity Pathways Analysis, included neural-related categories, whereas the ones associated with the downregulated genes included cellular movement, cell-to-cell signaling and interaction, and tissue and organismal development (Figure S1B). Moreover, we observed differential expression of several neuronal and neuroendocrine markers (*Ascl1* -Ash1-, *Elavl4*, *Syp*, *Ncam*), which were highly expressed in small cells, and of progenitor cell and mesenchymal markers (*Nestin*, *Vimentin*, *Sca1*, *Bmp4*, *Cd44*), which were highly expressed in large cells. Interestingly *Mycl1* and *Mycn* were overexpressed only in small cells. The

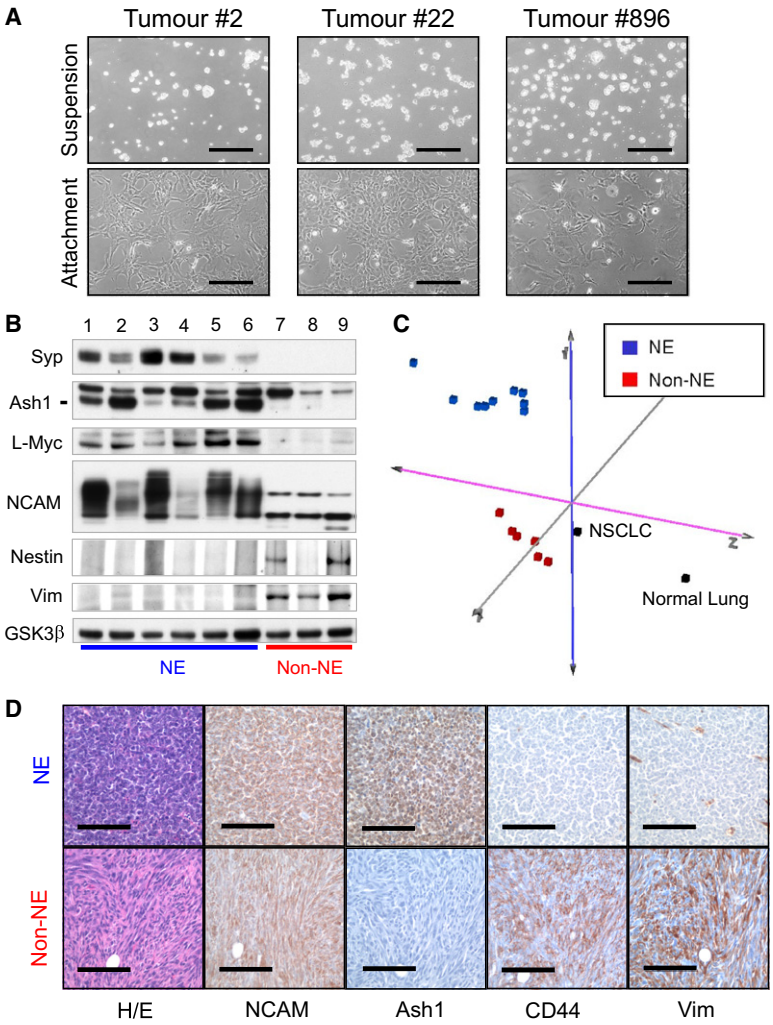

Figure 1. Phenotypic Variation in Cell Lines Derived from Mouse SCLC Tumors

(A) Photomicrographs showing the morphology of cells growing in suspending aggregates (upper panels) and of attaching cells featuring spindle-like shape (lower panels). Cell clones derived from tumors #2 (C2.04 and C2.20), #22 (C22.08 and C22.03), and #896 (C896.04 and C896.02) are shown. Scale bar, 100 μm.

(B) Western blot analysis of neuroendocrine markers (Syp1, Ash1, NCAM), L-Myc, mesenchymal markers (Nestin, Vimentin), and GSK3β (loading control) in six clones growing as suspending aggregates (lanes 1–6) and three clones growing as monolayer (lanes 7–9), derived from six different SCLC tumors (1:C9.05; 2:C2.04; 3:C18.04; 4:C22.08; 5:C4.06; 6:C788.01; 7:C22.03; 8:C4.05; 9:C788.06).

(C) PCA representing the sample similarities among the genome-wide expression profiles of nine clones growing as suspending aggregates (blue) and six clones growing attached (red); these clones had been derived from eight independent SCLC tumors (#2, #4, #9, #18, #22, #610, #788, and #896; each obtained from a different mouse). Normal lung and mouse NSCLC cells were used as controls (black).

(D) Photomicrographs showing the morphology (H/E staining) and immunophenotype of s.c. transplanted tumor cell clones growing as suspending aggregates (C896.04, upper pictures) and growing attached (C22.03, lower pictures). Immunohistochemistry was performed using specific antibodies against NCAM, Ash1, CD44, and Vimentin and developed with DAB (brown color).

Scale bar, 100 μm. See Tables S1 and S2 for a complete list of tumors in culture and derived cell lines, and Figure S1 for an extended expression analysis.

expression patterns of Nestin, Vimentin, and L-Myc (*Mycl1*) were confirmed by western blot (Figure 1B), and the surface expression of CD44 was confirmed by FACS analysis (Figure 2B).

Several clonal cell lines of each subtype (small, n = 8; large, n = 5) were injected subcutaneously (s.c.) into immunocompromised Balb/c *nu/nu* mice. Only cells with the small cell phenotype generated tumors with SCLC characteristics, whereas cells with large cell phenotype generated tumors with the large cell mesenchymal-like marker profile (Figure 1D). Interestingly, when these transplanted tumors were explanted and cultured in vitro, they appeared to have fully retained the small or large cell type features, indicating that neither cell type is capable of regenerating the heterogeneity seen in the primary tumor (data not shown). In view of these observations, cell clones with small cell, neuroendocrine phenotype were named neuroendocrine (NE) and the ones with large cell phenotype, lacking neuroendocrine marker expression, non-neuroendocrine (NonNE).

Presence of NonNE Cells in Primary Mouse SCLC and in Human SCLC Tumor Cell Lines

Immunohistochemistry performed on primary mouse SCLC tumors revealed the presence of variable amounts of dispersed CD44 positive cells. Some tumors contained almost no $CD44^+$ cells, whereas in other tumors small clusters of $CD44^+$ tumor cells were easily detected (Figure 2A). Although CD44 expression is found in various cell types and cannot be used as a unique marker for NonNE cells, clustered $CD44^+$ cells in SCLC tumors were considered transformed tumor cells because of their cytological characteristics. In support of this notion, cells with NonNE phenotype could be easily detected in the first passage of explanted, in vitro cultured tumors with relatively high $CD44^+$ staining (Figure 2C). Moreover, tumor cell suspensions containing both NE and NonNE cell populations could be expanded in vivo by s.c. injection into Balb/c *nu/nu* mice, for up to three passages, while retaining both cell populations (data not shown). In addition we obtained clonal cell lines from the NCI-H446 human cell line by FACS single $CD44^+$ and $CD44^-$ cells into 96-well plates. Their morphologies were consistent with the NonNE ($CD44^+$) and NE ($CD44^-$) phenotypes, respectively (Figure S2).

Clonal Relation of NE and NonNE Cell Lines

Next, we hypothesized that cell clones derived from a single mouse SCLC tumor might share similarly a common pattern of genetic aberrations, indicative for their clonal origin. SKY analysis performed on a NE and a NonNE subline obtained from a single mouse SCLC tumor was consistent with this hypothesis; similar translocations were observed in the two lines (Figures 3A; Figure S3). To confirm these results and obtain higher resolution

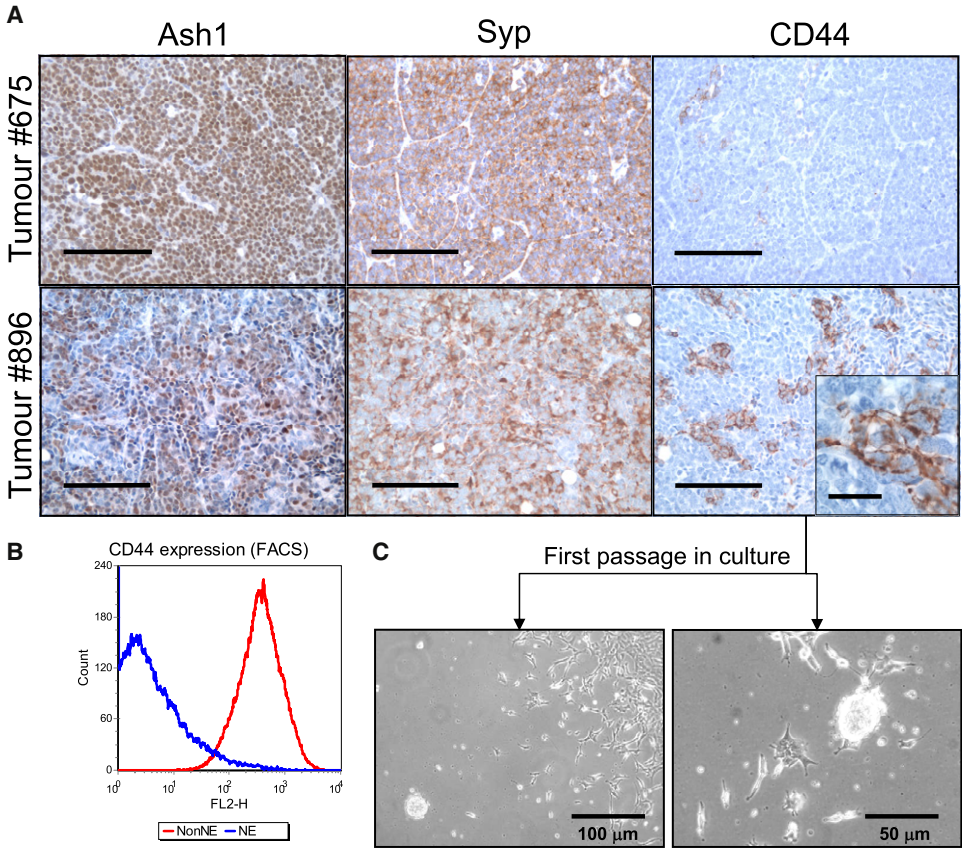

Figure 2. NonNE Cells Are Present in Primary SCLC Tumors

(A) Photomicrographs showing the detection in tumors #675 and #896 of Ash1 and Syp (NE cell markers) and CD44 (NonNE cell marker) by immunohistochemistry using specific antibodies and developed with DAB (brown color). Scale bar, 100 μm. Inset in the lower right panel shows a cluster of $CD44^{+}$ cells.

(B) Flow cytometric analysis of NE cells (C22.08, blue line) and NonNE cells (C22.03, red line) labeled with fluorochrome (PE)-conjugated anti-CD44 monoclonal antibodies.

(C) Phase-contrast photomicrographs showing cells with divergent morphological characteristics in primary culture of a SCLC tumor (#896, first in vitro passage, 7 days in culture).

See also Figure S2.

data, array-CGH analysis was performed using a 1 Mb resolution BAC array platform (Chung et al., 2004). Analyses were carried out on four pairs of clonal cell lines derived from four different tumors, and on material of the corresponding primary tumors. As expected, all cell lines and tumor samples showed copy number variations, although relatively few genetic aberrations were observed in each case. The most distinctive changes were found on chromosome 4. Importantly, cell clones derived from a single tumor shared some of the genetic aberrations, characterized by the boundaries of the amplicons, and level of copy number alteration. For instance, cell clones C22.08 (NE) and C22.03 (NonNE) derived from tumor #22 showed a common amplification near the end of chromosome 4, as well as a deleted area at the very end of chromosome 4. Similarly, cell clones C788.01 (NE) and C788.06 (NonNE) shared the amplification of regions on chromosome 4 (Figure 3B). Although these data confirmed the clonal origin for NE and NonNE cell clones derived from tumors #22 and #788, respectively, we could not define shared aberrations in NE and NonNE clones derived from tumor #4 or #610 using this method. At the same time, marked differences were also found in all pairs of cell lines. A severalfold amplification of a narrow region containing the *Mycl1* gene was found only in the cell lines with small cell phenotype, consistent with the L-Myc protein expression pattern observed by western blotting (Figure 1B).

Ras^{V12} Induces NE to NonNE Transition

It has been previously described that ectopic expression of oncogenic mutant HRas protein induces the transition of human SCLC cell lines to a dedifferentiated phenotype, characterized by the downregulation of neuroendocrine markers (Falco et al., 1990; Mabry et al., 1988). Therefore, we investigated whether Ras activation could drive the transition from NE to the NonNE phenotype in mouse SCLC clonal cell lines. Ras^{V12} was retrovirally transduced into three NE clonal cell lines derived from independent tumors. Although the initial response to oncogenic Ras expression was a reduction in cell proliferation, all the transduced cultures recovered and showed a transition to an adherent phenotype, with increased cell size and spreading (Figure 4A). Ectopic Ras expression also resulted in downregulation

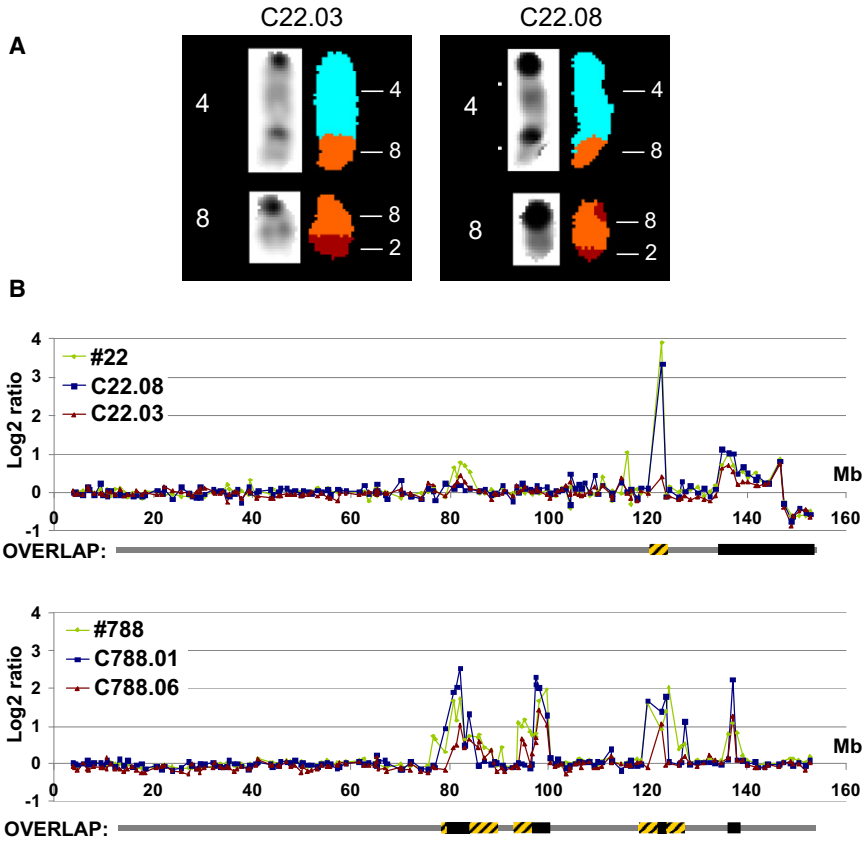

Figure 3. Clonal Genetic Alterations in Cell Variants Obtained from Single Tumors

(A) SKY analysis on the variant cell clones C22.03 NonNE and C22.08 NE obtained from tumor #22 revealed common clonal derivations involving chromosome 4 (der4/8) and chromosome 8 (der8/2). The results for the complete karyotype can be found in Figure S3.

(B) DNA from tumor #22 (upper plot, green line) and its derived cell variants C22.03 NonNE (red line) and C22.08 NE (blue line), and from tumor #788 (lower plot, green line) and its derived cell variants C788.01 NE (blue line) and C788.06 NonNE (red line) were subjected to array CGH analysis. Log2 signal ratios (tumor versus nontumor genomic DNA) for chromosome 4 are shown in the figure. In the underlying diagram (OVERLAP), chromosomal areas showing no copy number alterations are displayed with a gray bar. Areas of common DNA copy number changes (NE and NonNE cell variants) are displayed with black boxes, representing clonal genetic alterations. Areas of divergent DNA copy number changes (NE and NonNE cell variants) are displayed with yellow-black striped boxes.

of NE marker expression at the protein level, as shown for Syp and Ash1 (Figure 4B). Interestingly, a marked downregulation of L-myc protein expression was observed in Ras^{V12}-transduced cells. Moreover, genome-wide expression profiling showed profound changes in the transcriptome, and PCA confirmed a strong similarity between Ras^{V12}-transduced NE cells and NonNE cells, which clustered within the same 3D space and very well separated from nontransduced and empty vector-transduced NE cells (Figure 4C). The expression of the genes included in the NE versus NonNE signature was drastically modified by Ras^{V12} transduction (Figure 5B). A large fraction of the genes differentially expressed between NE and Ras^{V12}-transduced NE cells overlapped with the set of NE versus NonNE differentially expressed genes (505/743, Figure 5A). In order to narrow down the effects of Ras^{V12} expression directly related to the acquisition of the NonNE phenotype, we identified the most significant ($p < 0.005$) overexpressed genes included in this overlapping gene set (Figure 5C). Thirty genes were identified, including known mesenchymal markers (Vimentin, CD44) and several effectors of the Ras-MAPK pathway (c-Myc, Cyclin D1, Fra-1, RRas, MKP-3). In view of these results, we questioned whether the MAPK pathway was also activated in NonNE cells derived from SCLC tumors. Consistent phosphorylation (activation) of p42/p44 (Erk) was observed in all NonNE cells, but not in the NE cells tested (Figure S4A). However, sequence analysis of *K-Ras*, *H-Ras*, and *N-Ras* genes in seven SCLC-derived NonNE cell lines specifically looking for activating mutations at codon 12, 13, and 61 did not detect any activating mutation (Figure S4; data not shown). Finally, Ras^{V12}-transduced cells formed tumors of large, $CD44^{+}$, $Ash1^{-}$ cells when injected s.c. into Balb/c *nu/nu* mice (Figure 4D) and were undistinguishable from the tumors formed by NonNE cells directly isolated from primary SCLC (Figure 1D).

In Vitro Crosstalk

Next, we wondered whether there is any selection pressure to maintain cells with these divergent differentiation patterns in a tumor. To address this question we monitored the effects of coculturing and cografting both cell types in vitro and in vivo, respectively, with regard to proliferation and other tumor parameters. First, luciferase-labeled NE cells (C896.04) and NonNE cells (C22.03) were admixed in different ratios to define conditions in which the s.c. grafted mixtures would resemble the primary tumors with regard to the relative abundances of NE and NonNE cells. A ratio of four (NE) to one (NonNE) appeared to give a distribution resembling those of primary tumors with a relatively high NonNE component. In other studies in which the contribution of stromal cells to tumor cell behavior was assessed, a one (tumor cells) to three (stromal cells) ratio was used (Karnoub et al., 2007). We seeded the cells in the 4:1 ratio in serum-free medium (Figure 6A) and compared to nonmixed cells. NE cells showed a strong tendency to attach and spread on the NonNE cell monolayer, while maintaining their small size (Figure 6B). In fact, mixed cells grew as adherent, multilayered cultures; this in clear contrast to pure NE cell cultures (floating aggregates) and to NonNE cells (large cell monolayer). Cells were counted on days 3, 4, and 5 after seeding. Although both nonmixed NE and NonNE cultures had limited capacity to proliferate in serum-free conditions, admixed cells showed

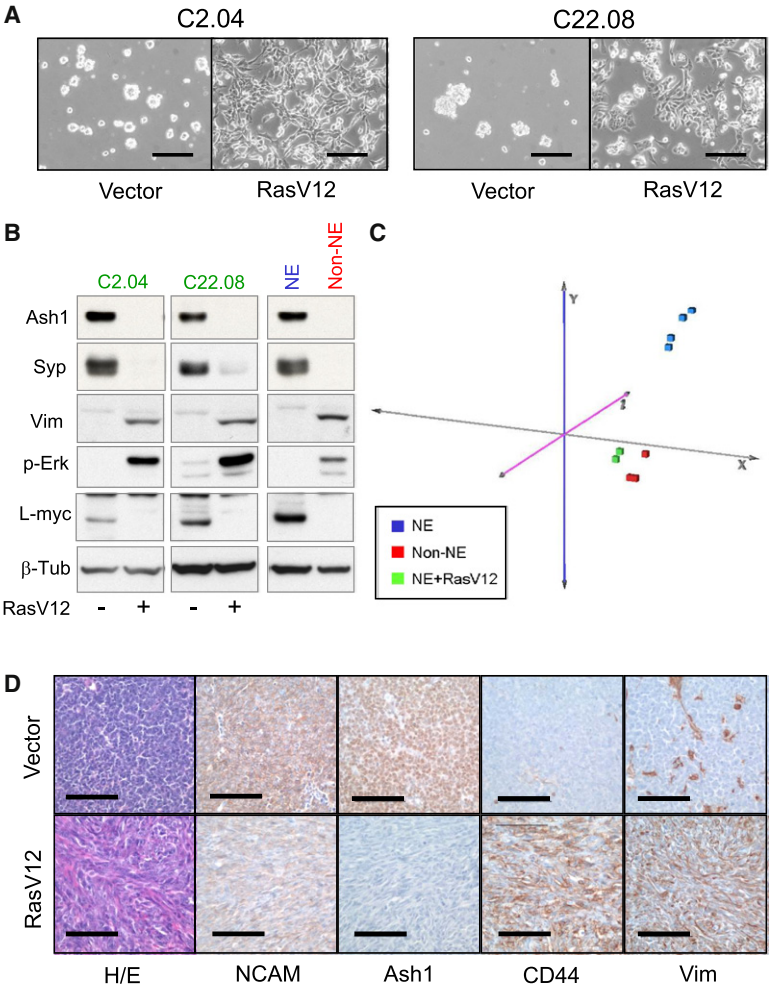

Figure 4. *Ras*^{V12}-Mediated Transition from NE to NonNE Phenotype

Cell clones with NE phenotype (C2.04, C22.08) derived from two independent tumors were retrovirally transduced with the *Ras*^{V12} gene and analyzed.

(A) Phase-contrast photomicrographs showing the morphology of *Ras*^{V12}-transduced and empty vector-infected cells. Scale bar, 100 μm.

(B) Western blot analysis for the detection of neuroendocrine markers (Syp1, Ash1), mesenchymal markers (Nestin, Vimentin), phospho-Erk1/2, and β-Tubulin (loading control) in NE cells transduced with the *Ras*^{V12} gene (+) or with the empty vector (–), as indicated. As controls, nontreated NE and NonNE cells are shown.

(C) PCA representing the sample similarities among the genome-wide expression profiles of three NonNE cell clones (red), two NE cell clones noninfected and empty-vector infected (blue), and the same two NE cell clones transduced with the *Ras*^{V12} gene (green).

(D) Photomicrographs showing the morphology (H/E staining) and immunophenotype of transplanted tumors obtained by injection of empty vector-infected cells (upper pictures) and of *Ras*^{V12}-transduced cells (lower pictures) into the s.c. tissue of immunocompromised mice. Immunohistochemistry was performed using specific antibodies against NCAM, Ash1, CD44, and Vimentin and developed with DAB (brown color). Scale bar, 100 μm.

See also Figure S4.

a 3- to 4-fold increase in cell number as compared to the sum of the individually seeded cultures at the time points shown (Figure 6C). Quantification of luciferase activity, only present in C896.04 NE cells and not in C22.03 NonNE cells, showed a 4-fold increment in admixed compared to nonmixed cells after 4 days in culture (Figure 6D), indicating that NE cells have a proliferation advantage when cultured in the presence of NonNE cells. The proportion of NonNE cells in the mixed culture was analyzed by FACS analysis using CD44 expression as a marker for NonNE cells (Figure 6E). A 2-fold relative increase in NonNE cell number in mixed culture compared to nonmixed cells was estimated on the basis of the percentage of CD44^{+} and total cell count, suggesting that NonNE cells may also benefit from the presence of NE cells in the culture, albeit to a lesser extent. The large difference in CD44 surface expression between NE and NonNE cells in admixed cultures also permitted purification of the different cell populations. Using magnetic beads and monoclonal antibodies against CD44, admixed cells cultured for 4 days were separated into CD44^{+} (NonNE) and CD44^{-} (NE) populations, with over 90% purity (Figure S5). The sorted cells were morphologically indistinguishable from the parental nonmixed populations, i.e., admixed, sorted NE cells grew as suspending aggregates, and NonNE cells as a monolayer.

In an attempt to define the molecular signals mediating the crosstalk between NE and NonNE cells, we analyzed secretion of several cytokines into the culturing medium using an antibody array. Cells were plated in serum-free medium for 2 days either as single populations or admixed, and culture supernatants were analyzed (Figure S6). No cytokines were detected in C896.04 NE and in C2.04 NE cell culture supernatants. C22.03 NonNE culture supernatant contained high levels of several cytokines, including CCL2 (MCP1), CCL5 (Rantes), CCL9 (MIP-1γ), CXCL1 (KC), CXCL5 (LIX), Selp (P-Selectin), and sTNFR1. Interestingly, culture supernatants of the admixed cell lines showed de novo secretion of IGFBP-3 and IGFBP-5. Moreover, the *Ras*^{V12}-mediated phenotypic transition in C2.04 NE cells was accompanied by the expression of several cytokines, mostly overlapping the cytokine expression profile observed in C22.03 NonNE cells (Figure S6).

In Vivo Grafting of NonNE and NE Mixtures Potentiates Metastasis

Coculturing NE and NonNE cells derived from mouse SCLC had dramatic effects on cell proliferation and morphology, but the physiological significance can only be evaluated properly in vivo. In parallel experiments, luciferase-labeled NE cells (C896.04) and NonNE cells (C22.03) were injected s.c. into immunocompromised mice either as single populations or admixed at a 4:1 ratio. Tumor growth was monitored by direct measurement of tumor diameter with a caliper. In contrast to what we observed in vitro, growth of admixed cell tumors was not significantly different from the growth of single tumor cell populations

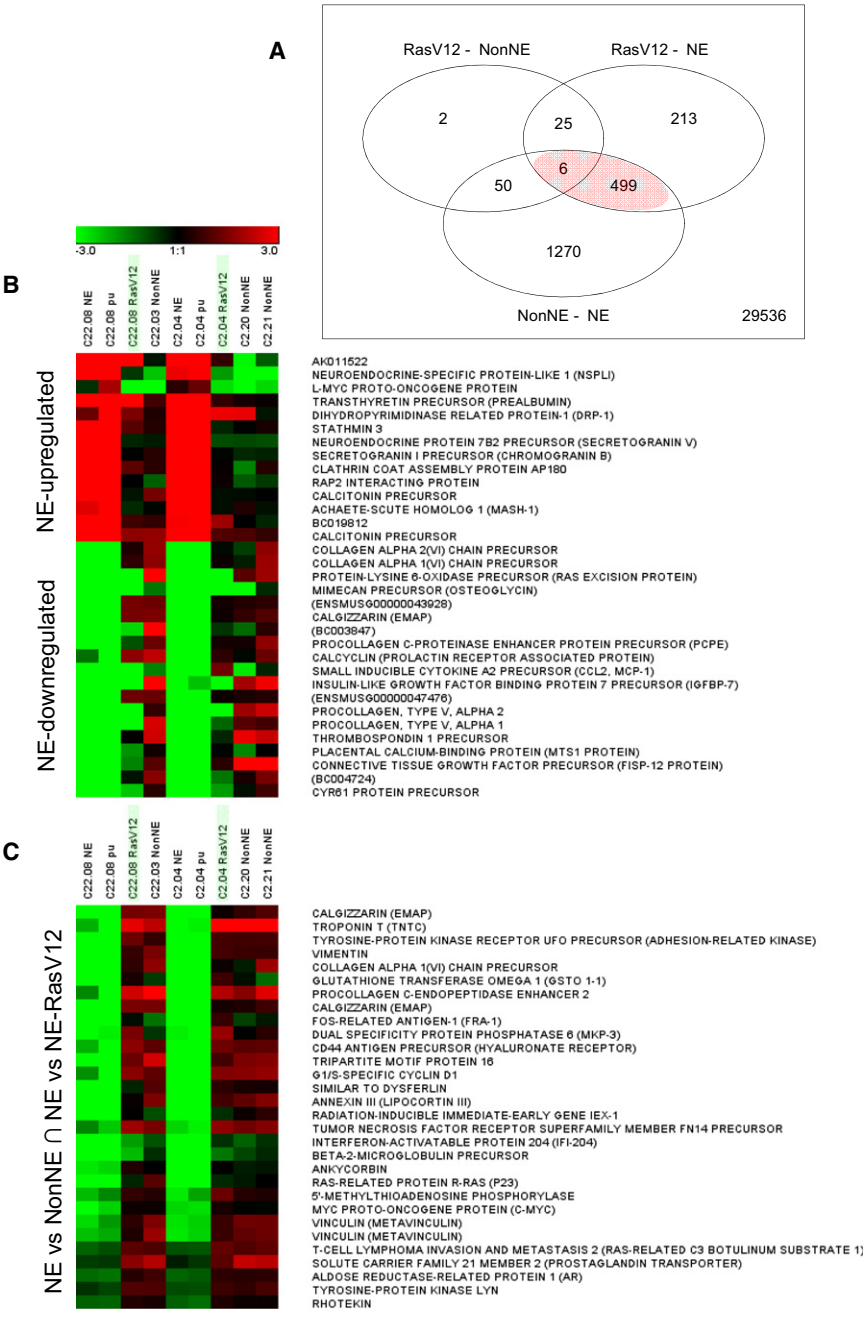

Figure 5. Oncogenic Mutant Ras Induces Dramatic Changes in Gene Expression

The expression profiles of three NonNE cell clones (C22.03, C2.20, and C2.21), two NE cell clones (C22.08 and C2.04), empty-vector infected NE cell clones (C22.08 p and C2.04 p), and the same two NE cell clones transduced with the Ras^{V12} gene (C22.08 RasV12 and C2.04 RasV12) were further analyzed to identify the differentially expressed genes.

(A) Venn diagram representing the numbers of differentially expressed genes in each indicated paired comparison set ($p < 0.05$), and the overlap between sets.

(B) Heat map representing the Ras^{V12}-induced variation in the expression of the genes included in the NE versus NonNE signature, as defined in Figure S1A.

(C) Heat map representing the expression values of the genes found overexpressed in both NonNE versus NE and RasV12 versus NE comparisons ($p < 0.005$), corresponding to the highlighted area in (A).

(Figure 7A). In fact, NonNE-only tumors showed early engraftment and slow growth, NE-only tumors showed rapid growth after a lag phase, and mixed-cell tumors showed early engraftment and intermediate growth rate (data not shown). The NE cell proliferation in single and mixed tumors was followed by luciferase imaging. Although no reproducible differences were observed in luciferase signals between these groups (data not shown), this method yielded an unexpected result. Mice injected s.c. with mixed populations of cells consistently exhibited a strong luciferase signal in the upper abdominal region; this in clear contrast with mice injected with NE cells only, which never showed any luciferase signal in the abdominal area (Figure 7B). Necropsies revealed the presence of extensive metastases in the liver of mice injected s.c. with admixed cells (Figure 7C), whereas mice injected with either NE or NonNE clonal cell lines showed no evidence for liver metastases. Careful histopathology and immunohistochemistry confirmed these results, i.e., the massive presence of metastatic lesions in the liver of mice injected s.c. with this combination of NE and NonNE clonal cell lines and their complete absence in mice grafted with only a single-cell population. Immunohistochemistry of the s.c. admixed tumors showed the presence of both $CD44^+$; $Ash1^-$ and $CD44^-$; $Ash1^+$ cells, distributed in patches. At the areas of contact between NE and NonNE populations, $CD44^+$ cells were found intermixed with $CD44^-$ cells (Figure 7C), resembling the distribution observed in primary mouse SCLC tumors with a relatively high fraction of NonNE cells (compare Figure 7C with Figure 2A). Metastatic lesions were found in the liver and in some cases in axillary lymph nodes, but not in lung or mediastinal lymph nodes. More importantly, metastatic lesions were constituted of NE-differentiated cells, with no evidence for the presence of NonNE cells. This is consistent with the high luciferase signal detected during in vivo imaging of the mice because the luciferase reporter was only present in the NE cells used in this experiment, and not in the NonNE cells. To confirm this observation, β-galactosidase-expressing C22.03 NonNE cells were admixed to C896.04 NE cells and injected s.c. into nude mice. Detection of

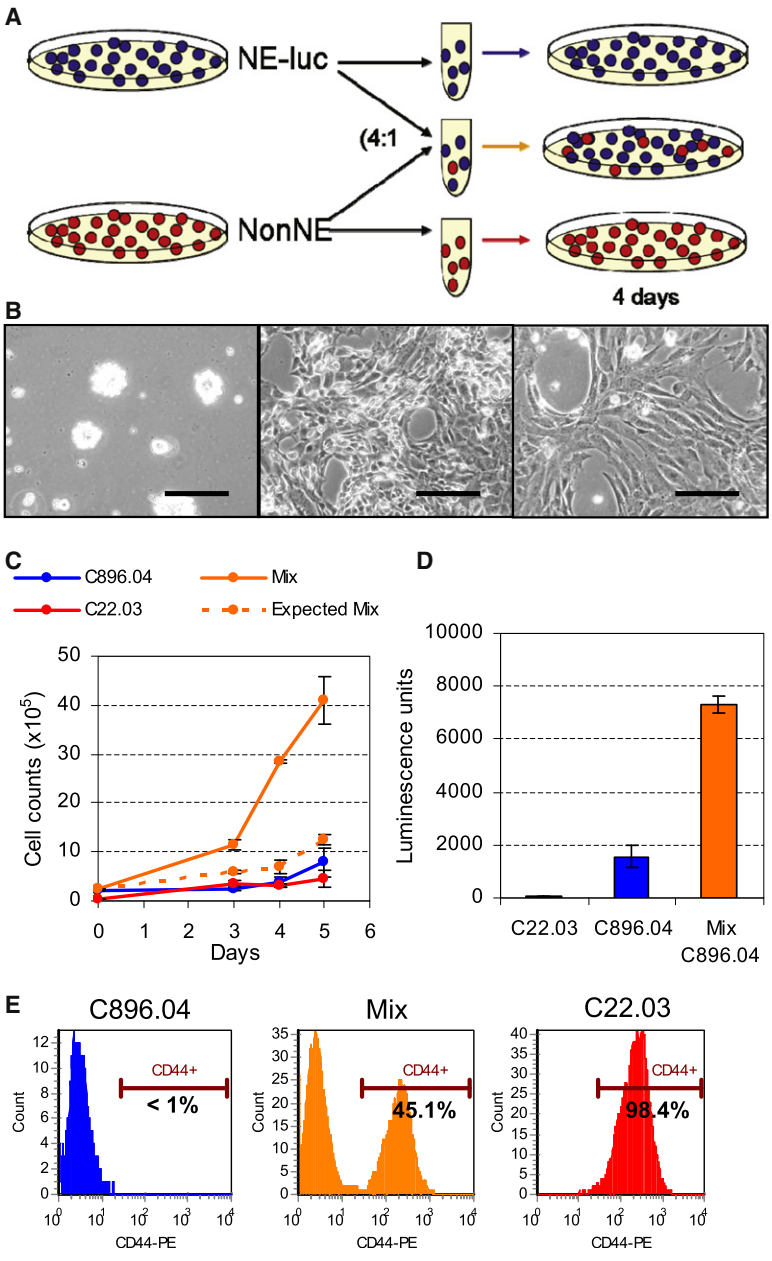

Figure 6. Increased Proliferation Rate and Morphological Change in Admixed NE/NonNE Cultures

Luciferase-expressing NE cells (C896.04) and NonNE cells (C22.03) were used.

(A) Schematic representation of the experimental design. NE-luc cells were admixed with NonNE cells at a 4:1 ratio, seeded in serum-free medium, and kept in culture for up to 5 days.

(B) Phase-contrast photomicrographs showing the morphology of pure NE culture (left), pure NonNE culture (right), and NE+NonNE mixed culture (middle). Scale bar, 50 μm.

(C) Cell proliferation curves showing the cell counts of pure NE culture (blue line), pure NonNE culture (red line), and NE+NonNE mixed culture (orange line). Dotted line represents the expected cell counts considering the summation of cell counts in NE and NonNE pure cultures.

(D) Bioluminescence measurement of pure NE cells (blue bar), pure NonNE cells (red bar), and mixed NE+NonNE cells (orange bar) after 4 days in culture. Note that only NE cells express luciferase. (E) Flow cytometric analysis of CD44 expression in pure NE culture (left, in blue), pure NonNE culture (right, in red), and mixed NE+NonNE culture (middle, in orange), 4 days after seeding. The quantification of $CD44^+$ cell (percentage) is shown.

Data are represented as mean ± SD. See also Figure S5.

β-galactosidase expression by immunohistochemistry showed clustered and interspersed C22.03 NonNE cells in the grafted tumors, but not in the liver metastasis, nor in the liver parenchyma (Figure 7D). The enhanced potential to metastasize was found to be a reproducible phenotype because it could be reproduced in three independent graft experiments, with an overall incidence of liver metastases of 17/18 mice injected with the admixed cell populations. In contrast, none of the six mice injected with C896.04 NE cells alone and of the six mice injected with C22.03 NonNE cells alone presented with liver metastases (Figure 7E). Combinations involving these and other cell lines (C2.20 NonNE, C788.06 NonNE, C610.01 NE, C2.04 NE) were also tested in the same system. Four of the combinations (C22.03/C896.04, C22.03/C2.04, C2.20/C896.04, and C2.20/C2.04) had a statistically significant increase in metastatic incidence ($p < 0.05$), when comparing NE cells injected alone or in combination with NonNE cells. The fact that some combinations gave a higher metastasis rate than others is likely due to different in vivo proliferation rates of each of the cell lines tested, changing the ratio between NE and NonNE cells in the tumor. The incidence of liver metastasis over all the combinations and experiments was 35 out of 53 mice, whereas none of 30 mice injected with single-cell populations showed distant spreading of tumor cells ($p < 0.05$). Altogether, these results indicate that the presence of NonNE cells in s.c. grafted tumors endows the NE cells with a dramatically enhanced ability to metastasize to the liver.

Next, we questioned whether enhanced metastatic potential was a systemic effect or required close contact between different cell populations. C896.04 NE cells were injected s.c. into the left and C22.03 NonNE into the right flank of the same immunocompromised animals. None of the seven animals injected with this combination of cells at contralateral flanks developed liver metastases, suggesting that close contact or vicinity of both cell populations within the same tumor is required to confer the metastatic potential to the NE cell population.

DISCUSSION

Mouse SCLC tumors share many features with human SCLC, including cellular morphology, marker profile, and pattern of metastatic spread to specific organs. Here, we show that mouse SCLC tumors are often composed of multiple tumor cell types: small NE cells and large NonNE cells with mesenchymal features. The derivation of cell lines with different cell morphologies from

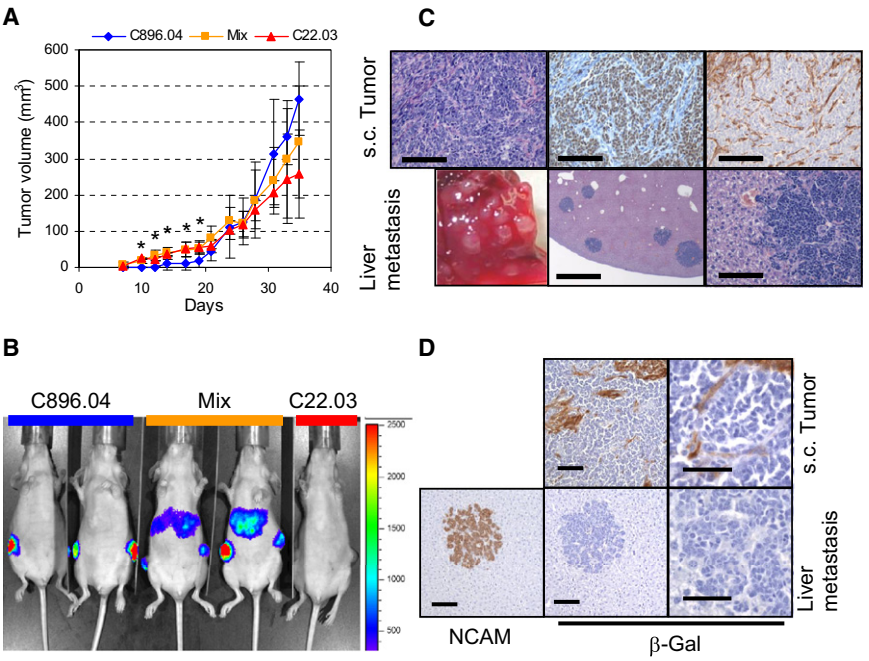

E

		NE cell lines			
		none	C896.04	C610.01	C2.04
NonNE cell lines	none		0/6	0/6	0/4
	C22.03	0/6	17/18 *	2#/8	5/8 *
	C2.20	0/6	6#/7 *	1/4	3/4 *
	C788.06	0/2	1/4	n.a.	n.a.
C22.03 (NonNE) at Right flank & C896.04 (NE) at Left flank: 0/7					

Metastases in axillary lymph nodes. * $p < 0.05$

Figure 7. Enhanced Metastatic Potential of NE Cells When Admixed to NonNE Cells in Graft Experiments

(A) Tumor volume measurement of transplanted tumors after injection of pure NE cells (C896.04, blue line), pure NonNE cells (C22.03, red line), or mixed NE+NonNE cells (orange line). Data are presented as mean ± SD; asterisks denote a volume difference between pure NE and pure NonNE tumors ($p < 0.05$).

(B) In vivo detection of luciferase reporter expression by bioluminescence imaging. NE cells (C896.04) were the only cells expressing luciferase. In this picture, two mice injected into both flanks with pure NE cells (blue line, left), one mouse injected into both flanks with pure NonNE cells (red line, right), and two mice injected with mixed NE+NonNE cells (orange line, middle) are shown.

(C) Upper panels show the morphology (H/E staining, left) and the expression of Ash1 (middle) and CD44 (right) by immunochemistry (DAB, brown color) of a subcutaneously transplanted tumor after injection of NE+NonNE mixed cells. Scale bars, 100 μm. Lower panels show the extensive metastatic colonization of the liver in mice injected s.c. with mixed NE+NonNE cells.

(D) Detection of β-gal expressing C22.03 cells (NonNE) by immunohistochemistry (DAB, brown color) in the subcutaneously transplanted tumors and metastases (two upper and two lower-right photomicrographs, respectively) after injection of mixed NE+NonNE cells. In the same mouse, liver metastases were stained positive for NCAM (lower left). Scale bars, 100 μm (low magnification) and 20 μm (high magnification).

(E) Frequency of metastases in Balb/c Nude mice injected with either pure NE cells, pure NonNE cells, or the NE+NonNE mix, as indicated. The frequency is expressed as number of mice with liver metastases/number of mice in that group. # indicates the detection of lymph node metastasis in mice lacking liver metastases. Asterisks denote statistical significance (chi-square test) with $p < 0.05$. See also Figure S6.

human SCLC tumors has also been reported (Carney et al., 1985a, 1985b). However, the procedures for deriving these cell lines might have limited the persistence of heterogeneous cultures to rare cases, either because culture conditions selected for specific variants or because cell lines were derived from metastatic locations that exclusively were composed of tumor cells with neuroendocrine characteristics. Interestingly, the NCI-H446 SCLC human cell line can be propagated as a mixture of adherent and suspending cells, and these populations can be separated based on differential adherence to substrate (Doyle et al., 1990). It is important to point out that the phenotypically different cell variants isolated from individual murine (this work) and human tumors (Doyle et al., 1990; Watanabe et al., 1988) are often of clonal origin but show significant differences at the genetic level. Our results using SCLC cell lines are in agreement with those of Watanabe and collaborators (Watanabe et al., 1988), who reported that several chromosomal markers were shared by the different human SCLC sublines, whereas *MYCL1* amplification was only present in the two sublines expressing neuroendocrine antigens. This conforms to the notion that in general, tumors originate from a single cell that undergoes a repetitive process of mutation, selection, and expansion (Figure 8). During this process new cell variants arise, and some of them, most likely "the fittest," will expand, whereas others are lost. However, variant clones with similar fitness but with properties for which no selection is imposed will persist and contribute to the genetic diversity of the tumor. From the viewpoint of population genetics, genetic variability is an advantageous feature because it better permits adaptation to changes in the environment. Tumor heterogeneity easily results from chromosomal instability or DNA repair defects, which are hallmarks of tumor cells. This might also permit the concomitant selection within the same tumor of cell clones that coevolve with mutual dependencies, giving rise to a tumor tissue in which the different tumor cell clones fulfill their own specific function. The recurrent presence, in independent tumors, of neuroendocrine and NonNE tumor cell clones is a remarkable demonstration of such coevolution process. We speculated that the coexistence of NE and NonNE cells in a tumor confers a selective advantage to the tumor as a whole.

We show here that within largely neuroendocrine SCLC tumors, variant tumor cell clones can be found that lack

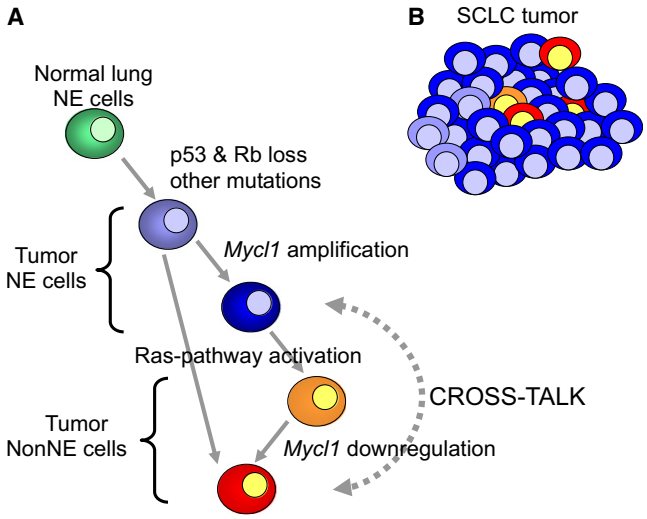

Figure 8. Generation of Functional Cell Heterogeneity in SCLC Tumors

The model describes the sequence of events that might create cell heterogeneity with a functional role in SCLC tumors, in line with our observations.

(A) Tumor cell progression is driven by a repeated cycle of mutation, cell expansion, and natural selection. In the mouse SCLC tumor model used here, *Trp53* and *Rb1* deletions initiate the tumorigenic process. Genetic instability is the driving force facilitating accumulation of new mutations and generating genetic variability within the tumor mass. *Mycl1* amplification might be a relevant progression step for NE cells in SCLC tumor because this is the most common spontaneous genetic alteration observed in mouse SCLC tumors. NonNE variants may originate from NE tumor cells upon activation of the Ras-signaling pathway. Oncogenic Ras expression in NE cells may block the expression of L-myc. The genetic variants present in a tumor are under continuous evolutionary pressures resulting in the selection of the fittest variants. This includes advantageous properties conferred by paracrine signaling leading to coevolutionary selection of subclones.

(B) As a consequence of the processes described in (A), SCLC tumors are composed of highly progressed NE cells (dark blue), and other variant cell lineages, representing less progressed NE cells (light blue) or NonNE cells (red). The tumor as a whole has a neuroendocrine phenotype ("looks blue") but harbors cell variants that convey specific tumor features.

neuroendocrine differentiation and express mesenchymal markers. As mentioned before, similar NonNE cell variants were previously described in a few human SCLC cell lines (Doyle et al., 1990; Watanabe et al., 1988), but neither of these reports questioned how these variants were generated nor did they address the possible consequences for the SCLC tumor. Other groups studied oncogenic-Ras-induced dedifferentiation of human SCLC cell lines and interpreted it as a progression event related to the occasional transition from a SCLC to a NSCLC phenotype in relapsed tumors. Our experiments indicate that expression of oncogenic Ras in mouse SCLC cell lines with a NE phenotype is sufficient to cause the transition to the NonNE phenotype. *Ras*-transduced cells silence the expression of NE markers and upregulate the expression of Vimentin and CD44, thereby imposing a NE to mesenchymal transition. Because introduction of mutant Ras into L-myc expressing NE cells resulted in cells in which L-myc expression was lost, the NonNE cells as found in the primary tumors could arise from preexisting NE cells that either did or did not carry a *Mycl1* amplification (Figure 8). Our results suggest that spontaneous transition to the NonNE phenotype requires activation of the MAPK pathway, although no Ras-activating mutations have been found in NonNE cell lines. Identification of the mutations that activate the MAPK pathway in the specific genetic context of neuroendocrine tumor cells will be addressed in future work. Furthermore, we cannot exclude the possibility that NE cells have arisen from progenitor cells with NonNE features, by the expression of factors, such as *Ascl1*, promoting neuroendocrine differentiation. *Ascl1* has recently been shown to collaborate with other factors in the conversion of fibroblasts into neurons (Vierbuchen et al., 2010). Whatever the precise route, we qualify this tumor cell diversification as a progression step that confers new malignant capacities to the tumor.

By setting up in vitro and in vivo mixing experiments, we observed synergistic effects on in vitro proliferation. In vivo, an unexpected enhancement of the metastatic potential of the NE cells was observed. The apparent discrepancy between the in vitro and in vivo proliferation capacity points to the existence of a limiting factor in the culture medium that becomes irrelevant in the context of grafted cells. Nonetheless, both systems illuminate the crosstalk between these tumor cell variants. EMT transitions have been described in detail in development, where they contribute to the plasticity required for the (re-)organization of tissues. They can fulfill a similar role in tumor progression by facilitating tumor cell invasion and metastasis (Polyak and Weinberg, 2009). In carcinomas, mesenchymal transitions can originate from microenvironmental signals or from (epi-)genetic changes. However, the precise mechanisms by which tumor cells with mesenchymal traits contribute to the consecutive steps resulting in colonization of distant organs by tumor cells are still largely unknown. The fact that most (if not all) metastases from epithelial carcinomas show epithelial differentiation at the metastatic site seems at odds with the observation that carcinomas that undergo EMT have an enhanced metastatic capacity. Two possible explanations have been proposed (Polyak and Weinberg, 2009). Tumor cells that underwent EMT in the primary tumor disseminate and seed distant organs where they undergo a mesenchymal to epithelial transition (MET), thereby regaining epithelial features. Alternatively, there could be a functional cooperation between mesenchymal and epithelial cells that potentiates the epithelial cells to metastasize, e.g., by the formation of mixed cell clumps that together better survive in the circulation (Hart, 2009) and/or by direct signaling (Lyons et al., 2008).

Considering that the NE to NonNE transition in neuroendocrine SCLC tumors parallels the EMT processes described for epithelial carcinomas, our results conform to the latter mechanism. Indeed, NonNE cells in the tumor grafts enhance the capacity of NE cells to metastasize, whereas NonNE cells do not metastasize in either mixed or nonmixed tumors. A similar case of cell cooperativity in metastasis involving EMT transition on hamster cheek pouch carcinoma-1 cells (HCPC-1) has been recently reported (Tsuji et al., 2008, 2009). Our results also indicate that neuroendocrine to mesenchymal transition in SCLC is a rare event that requires profound (genetic) changes that are not easily reverted because: (1) in all cases tested, NE and NonNE clones from a particular SCLC tumor present with marked differences in their CGH profile; (2) cloned NE and NonNE cell lines maintain their phenotype over a large number of passages in culture; and (3) forced transition from NE to NonNE phenotype was accomplished by overexpressing mutated Ras^{V12} protein and

after recovery of the cells from the initial Ras^{V12}-induced crisis. These data outline a scenario in which tumor cells converted to a mesenchymal phenotype by mutation and selection, create together with the NE cells a tumor microenvironment that is advantageous for both cell types, thereby securing their retention in the tumor. Evidently, increased metastatic potential cannot be by itself the driving force commanding retention or expansion of NonNE cells in SCLC tumors and, thereby, heterogeneity. However, mesenchymally differentiated tumor cells could participate in the reorganization of the tumor tissue as it has been described for EMT-affected cells in carcinomas, in several different ways: increasing motility and invasiveness, offering survival signals to other tumor cells, producing extracellular matrix and proteases, inducing inflammation, and promoting vascularization. Increased metastatic potential could be a by-product of one or several of these changes. It has been reported that mesenchymal stem cells enhance the metastatic potential of breast cancer cells at least in part by expressing the chemokine CCL5 (also known as Rantes). We have studied the expression of several chemokines in NE, NonNE, and mixed populations in vitro. Interestingly, CCL5 is expressed by NonNE cells whether or not they are admixed to NE cells. Still, several other cytokines are constitutively expressed by NonNE cells. Some of those are known to be proinflammatory and/or to contribute to the metastatic process in other systems.

In summary, our work presented here describes a specific type of tumor heterogeneity, in which the interaction between clonally derived but diversified subclones alters the behavior of the tumor as a whole. One of the outcomes is a substantially increased metastatic potential, a feature with important clinical ramifications. It makes us aware of the fact that tumor heterogeneity can have profound functional consequences. Tumor cell behavior then not only depends on the interactions with stromal cells but is also influenced by interactions with tumor cell variants that fulfill a distinct role in the tumor tissue. Enhanced metastatic capacity serves as an illustrative example of crosstalk between specialized tumor cell clones. Disrupting the paracrine signaling involved in this interaction is worth further exploring as a strategy to mitigate tumor progression.

EXPERIMENTAL PROCEDURES

A detailed description of the materials and methods utilized in this work can be found in the available online Supplemental Experimental Procedures.

Mouse Model for SCLC

All experiments involving animals comply with local and international regulations and ethical guidelines, and have been authorized by our local experimental animal committee at The Netherlands Cancer Institute (DEC-NKI). We have used the mouse model for SCLC described previously (Meuwissen et al., 2003). Compound $Trp53^{F2\text{-}10/\ F2\text{-}10}$;$Rb1^{F19/F19}$ and $Trp53^{F2\text{-}10/\ F2\text{-}10}$;$Rb1^{F19/F19}$;*LucR* (Kazarian et al., 2009) were induced by intratracheal delivery of 10^8 Ad5-CMV-Cre viral particles. When moribund, mice were sacrificed by CO_2; tumors were excised and processed for further analysis.

Derivation of Cell Lines and Ras^{V12} Transduction

Excised tumors were mechanically disaggregated with a sterile blade, cleared from large aggregates, washed with PBS, and seeded in modified HITES medium. To split cell cultures, suspending aggregates were harvested and mechanically disaggregated by pipetting up and down with a p200 micropipette. Adherent cultures were washed (PBS) and detached by incubating the cells in Trypsin (Invitrogen) for 5 min at room temperature. Clonal cell lines were derived from these cultures by preparing single-cell suspensions, passing them through a 40 μm sieve, and seeding them at different densities in soft-agar plates. Ras^{V12} transduction was performed using pBABE-puro-Ras^{V12} retroviruses with empty vector pBABE-puro retroviruses as control (Peeper et al., 2001), followed by a 72-hr selection in medium containing puromycin (Sigma).

WB Analysis

Protein separation and immunodetection (western blot) was performed as previously described with minimal changes (Calbo et al., 2002). We used the following primary antibodies against: Syp (rabbit polyclonal; Dako); Ash1 (mouse monoclonal; BD Biosciences); L-Myc (H-44, rabbit polyclonal; Santa Cruz); NCAM (Rabbit polyclonal; Chemicon); Nestin (mouse monoclonal; BD Biosciences), Vimentin (mouse monoclonal; BD Biosciences); and p-Erk (rabbit monoclonal; Cell Signaling). GSK-3β (rabbit polyclonal; Santa Cruz) and β-tubulin (mouse monoclonal; Klinipath) served as loading controls.

Histology and Immunohistochemistry

Formalin-fixed, paraffin-embedded tissues were cut into 4 μm sections and deposited on glass slides. For histological analysis, tissue sections were stained with hematoxylin and eosin (H/E). For immunohistochemistry, tissues were rehydrated, blocked in BSA containing PBS, and sequentially incubated with specific primary antibodies and with biotinylated secondary antibodies. For visualization we used streptABComplex (Dako) and diaminobenzidine (Dako) as a chromogen, following the instructions of the provider. Hematoxylin was used as a counterstain. The following antibodies were used against: NCAM (Rabbit polyclonal; Chemicon); Ash1 (mouse monoclonal; BD Biosciences); CD44 (rat monoclonal clone IM7; Santa Cruz); Vimentin (guinea pig polyclonal; RDI Fitzgerald Industries); Syp (mouse monoclonal clone SY38; Dako); and β-gal (rabbit monoclonal; Invitrogen). Biotinylated GoatαRab, GoatαMouse, RabbitαRat (all from Dako), and GoatαGuinea pig (Jackson Laboratories) were used as secondary antibodies.

CGH Analysis

DNA was either isolated as described previously (Jongsma et al., 2008) or using a Puregene DNA isolation kit following the manufacturer's instructions. All hybridizations were performed as previously described (Shakhova et al., 2006). For mouse genome information we used the Ensembl mouse genome server (v46, August 2007) based on the National Center for Biotechnology Information m36 mouse assembly (freeze May 08, 2006, strain C57BL/6J).

SKY Analysis

Metaphase preparations were hybridized using the mouse SkyPaint probe mixture (Applied Spectral Imaging, Migdal Ha'Emek, Israel) according to the manufacturer's instructions and mounted in 4′,6-diamidino-2-phenylindole/antifade solution. Using the SpectraCube 200 system and the skyview analysis software (Applied Spectral Imaging), eight to ten metaphases from each mSCLC clonal cell line were examined.

Expression Analysis and PCA

A 32K mouse oligoarray (Operon Biotechnologies, Inc.) was used for the relative quantification of mRNA expression profile, taking the Universal Mouse reference RNA (Stratagene) as reference. Results were then subjected to PCA from experiments using the Genesis Software (Institute for Genomics and Bioinformatics, Graz University of Technology, Graz, Austria [IGB-TUG]).

Transplantation of Cell Lines

Balb/c Nude immunosuppressed mice were used for s.c. transplantation of tumor cell lines. Injections of cells were performed in both flanks. Cell lines were injected as single-cell suspensions either as pure populations (NE 5×10^5 cells, NonNE 1×10^5) or mixed at a ratio 4:1 (NE 4×10^5 + NonNE 1×10^5 cells). Subcutaneously injected Balb/c nude mice were imaged on the IVIS200 (CCD camera; Biocompare) once a week. Tumors were allowed to

grow until a maximum volume of 1500 mm^3, and then mice where euthanized and tumors processed for further analysis.

ACCESSION NUMBERS

CGH array and expression array data have been deposited in the public database ArrayExpress (E-NCMF-36 and E-NCMF-37, respectively).

SUPPLEMENTAL INFORMATION

Supplemental Information includes Supplemental Experimental Procedures, six figures, and two tables and can be found with this article online at doi:10.1016/j.ccr.2010.12.021.

ACKNOWLEDGMENTS

We thank J. Zevenhoven and F. van de Ahé for their technical assistance; O. van Tellingen for setting up transplantation systems; R. Kerkhoven and A. Velds for their expert help with performing microarray analysis and interpreting the data; J. Song for her expert histopathology opinion; the personnel of the animal facility for taking excellent care of the mice; and P. Krimpenfort and K. Sutherland for critically reading the manuscript. We acknowledge D. Peeper for providing us with pBABE-puro constructs and S.T. Pals for providing us with several anti-CD44 antibodies. This work was supported by a grant of the Dutch Cancer Society.

Received: March 8, 2010
Revised: August 25, 2010
Accepted: November 17, 2010
Published: February 14, 2011

REFERENCES

Abeloff, M.D., Eggleston, J.C., Mendelsohn, G., Ettinger, D.S., and Baylin, S.B. (1979). Changes in morphologic and biochemical characteristics of small cell carcinoma of the lung. A clinicopathologic study. Am. J. Med. *66*, 757–764.

Calbo, J., Parreno, M., Sotillo, E., Yong, T., Mazo, A., Garriga, J., and Grana, X. (2002). G. cyclin/cyclin-dependent kinase-coordinated phosphorylation of endogenous pocket proteins differentially regulates their interactions with E2F4 and E2F1 and gene expression. J. Biol. Chem. *277*, 50263–50274.

Calbo, J., Meuwissen, R., van Montfort, E., van Tellingen, O., and Berns, A. (2005). Genotype-phenotype relationships in a mouse model for human small-cell lung cancer. Cold Spring Harb. Symp. Quant. Biol. *70*, 225–232.

Campbell, L.L., and Polyak, K. (2007). Breast tumor heterogeneity: cancer stem cells or clonal evolution? Cell Cycle *6*, 2332–2338.

Carney, D.N., Gazdar, A.F., Bepler, G., Guccion, J.G., Marangos, P.J., Moody, T.W., Zweig, M.H., and Minna, J.D. (1985a). Establishment and identification of small cell lung cancer cell lines having classic and variant features. Cancer Res. *45*, 2913–2923.

Carney, D.N., Gazdar, A.F., Nau, M., and Minna, J.D. (1985b). Biological heterogeneity of small cell lung cancer. Semin. Oncol. *12*, 289–303.

Chung, Y.J., Jonkers, J., Kitson, H., Fiegler, H., Humphray, S., Scott, C., Hunt, S., Yu, Y., Nishijima, I., Velds, A., et al. (2004). A whole-genome mouse BAC microarray with 1-Mb resolution for analysis of DNA copy number changes by array comparative genomic hybridization. Genome Res. *14*, 188–196.

Condeelis, J., and Pollard, J.W. (2006). Macrophages: obligate partners for tumor cell migration, invasion, and metastasis. Cell *124*, 263–266.

de Visser, K.E., Eichten, A., and Coussens, L.M. (2006). Paradoxical roles of the immune system during cancer development. Nat. Rev. Cancer *6*, 24–37.

Doyle, L.A., Borges, M., Hussain, A., Elias, A., and Tomiyasu, T. (1990). An adherent subline of a unique small-cell lung cancer cell line downregulates antigens of the neural cell adhesion molecule. J. Clin. Invest. *86*, 1848–1854.

Falco, J.P., Baylin, S.B., Lupu, R., Borges, M., Nelkin, B.D., Jasti, R.K., Davidson, N.E., and Mabry, M. (1990). v-rasH induces non-small cell phenotype, with associated growth factors and receptors, in a small cell lung cancer cell line. J. Clin. Invest. *85*, 1740–1745.

Gangemi, R., Paleari, L., Orengo, A.M., Cesario, A., Chessa, L., Ferrini, S., and Russo, P. (2009). Cancer stem cells: a new paradigm for understanding tumor growth and progression and drug resistance. Curr. Med. Chem. *16*, 1688–1703.

Hart, I.R. (2009). New evidence for tumour embolism as a mode of metastasis. J. Pathol. *219*, 275–276.

Heppner, G.H. (1984). Tumor heterogeneity. Cancer Res. *44*, 2259–2265.

Heppner, G.H. (1993). Cancer cell societies and tumor progression. Stem Cells *11*, 199–203.

Hildebrandt, H., Mühlenhoff, M., and Gerardy-Schahn, R. (2008). Polysialylation of NCAM. Neurochem. Res. in press. Published online May 7, 2008.

Jackman, D.M., and Johnson, B.E. (2005). Small-cell lung cancer. Lancet *366*, 1385–1396.

Jongsma, J., van Montfort, E., Vooijs, M., Zevenhoven, J., Krimpenfort, P., van der Valk, M., van de Vijver, M., and Berns, A. (2008). A conditional mouse model for malignant mesothelioma. Cancer Cell *13*, 261–271.

Kalluri, R., and Zeisberg, M. (2006). Fibroblasts in cancer. Nat. Rev. Cancer *6*, 392–401.

Karnoub, A.E., Dash, A.B., Vo, A.P., Sullivan, A., Brooks, M.W., Bell, G.W., Richardson, A.L., Polyak, K., Tubo, R., and Weinberg, R.A. (2007). Mesenchymal stem cells within tumour stroma promote breast cancer metastasis. Nature *449*, 557–563.

Kazarian, M., Calbo, J., Proost, N., Carpenter, C.L., Berns, A., and Laird-Offringa, I.A. (2009). Immune response in lung cancer mouse model mimics human anti-Hu reactivity. J. Neuroimmunol. *217*, 38–45.

Lantuejoul, S., Moro, D., Michalides, R.J., Brambilla, C., and Brambilla, E. (1998). Neural cell adhesion molecules (NCAM) and NCAM-PSA expression in neuroendocrine lung tumors. Am. J. Surg. Pathol. *22*, 1267–1276.

Linnoila, R.I., Gazdar, A.F., Funa, K., and Becker, K.L. (1993). Long-term selective culture of hamster pulmonary endocrine cells. Anat. Rec. *236*, 231–240.

Lyons, J.G., Lobo, E., Martorana, A.M., and Myerscough, M.R. (2008). Clonal diversity in carcinomas: its implications for tumour progression and the contribution made to it by epithelial-mesenchymal transitions. Clin. Exp. Metastasis *25*, 665–677.

Mabry, M., Nakagawa, T., Nelkin, B.D., McDowell, E., Gesell, M., Eggleston, J.C., Casero, R.A., Jr., and Baylin, S.B. (1988). v-Ha-ras oncogene insertion: a model for tumor progression of human small cell lung cancer. Proc. Natl. Acad. Sci. USA *85*, 6523–6527.

Meuwissen, R., Linn, S.C., Linnoila, R.I., Zevenhoven, J., Mooi, W.J., and Berns, A. (2003). Induction of small cell lung cancer by somatic inactivation of both Trp53 and Rb1 in a conditional mouse model. Cancer Cell *4*, 181–189.

Minna, J.D., Kurie, J.M., and Jacks, T. (2003). A big step in the study of small cell lung cancer. Cancer Cell *4*, 163–166.

Peeper, D.S., Dannenberg, J.H., Douma, S., te Riele, H., and Bernards, R. (2001). Escape from premature senescence is not sufficient for oncogenic transformation by Ras. Nat. Cell Biol. *3*, 198–203.

Polyak, K., and Weinberg, R.A. (2009). Transitions between epithelial and mesenchymal states: acquisition of malignant and stem cell traits. Nat. Rev. Cancer *9*, 265–273.

Rosen, J.M., and Jordan, C.T. (2009). The increasing complexity of the cancer stem cell paradigm. Science *324*, 1670–1673.

Shakhova, O., Leung, C., van Montfort, E., Berns, A., and Marino, S. (2006). Lack of Rb and p53 delays cerebellar development and predisposes to large cell anaplastic medulloblastoma through amplification of N-Myc and Ptch2. Cancer Res. *66*, 5190–5200.

Tsuji, T., Ibaragi, S., Shima, K., Hu, M.G., Katsurano, M., Sasaki, A., and Hu, G.F. (2008). Epithelial-mesenchymal transition induced by growth suppressor

p12CDK2-AP1 promotes tumor cell local invasion but suppresses distant colony growth. Cancer Res. *68*, 10377–10386.

Tsuji, T., Ibaragi, S., and Hu, G.F. (2009). Epithelial-mesenchymal transition and cell cooperativity in metastasis. Cancer Res. *69*, 7135–7139.

Vierbuchen, T., Ostermeier, A., Pang, Z.P., Kokubu, Y., Sudhof, T.C., and Wernig, M. (2010). Direct conversion of fibroblasts to functional neurons by defined factors. Nature *463*, 1035–1041.

Visvader, J.E., and Lindeman, G.J. (2008). Cancer stem cells in solid tumours: accumulating evidence and unresolved questions. Nat. Rev. Cancer *8*, 755–768.

Watanabe, H., Takahashi, T., Ueda, R., Utsumi, K.R., Sato, T., Ariyoshi, Y., Ota, K., Obata, Y., and Takahashi, T. (1988). Antigenic phenotype and biological characteristics of two distinct sublines derived from a small cell lung carcinoma cell line. Cancer Res. *48*, 2544–2549.